

Intrinsic emission spectra of bulk InP

Oleg Semyonov, Arsen Subashiev,* Zhichao Chen, and Serge Luryi

*Department of Electrical and Computer Engineering,
State University of New York at Stony Brook, Stony Brook, NY, 11794-2350*

The shape of the photoluminescence line excited at an edge face of InP wafer and registered from the broadside is used to investigate the intrinsic emission spectrum. The procedure is much less sensitive to the surface properties and the carrier kinetics than the conventional methods used with the reflection or transmission geometry of photoluminescence. Our method provides a tool for studying the effects of non-equilibrium distribution of minority carriers in doped direct-band semiconductors.

Keywords: photoluminescence, intrinsic emission, interband absorption, Urbach tail, doping fluctuations

INTRODUCTION

Luminescence spectroscopy of optically excited semiconductors is widely used for characterization of semiconductor materials¹, as well as for studying effects associated with the impurity levels², doping³, minority carrier kinetics⁴, varying composition and level quantization in quantum wells⁵. All these studies rely on the assumed knowledge or a possibility to determine the intrinsic emission spectrum produced in radiative recombination. For epitaxially grown submicron or quantum-well layers, the observed spectra are reasonably close to the intrinsic emission spectra (see Ref.⁶ for a discussion) and their interpretation is unambiguous.

The situation is different for bulk wafers, where the emission intensity and spectra are often influenced by technological defects of poorly controlled concentration. Moreover, the interpretation of bulk experimental spectra is also less straightforward. The observed spectra are modified by spectral filtering due to the wavelength-dependent reabsorption of the outgoing radiation in its propagation to the crystal surface^{7–9}. The reabsorption process strongly modifies the blue wing of the emission spectrum (where the absorption is very high) and results in a noticeable red shift of the emission maximum. Therefore, the spectra are sensitive to the minority carrier distribution in the sample, which in its turn depends on the carrier kinetics and surface effects.

For normal diffusion, the distribution is exponential and is determined by the hole generation profile (details of optical pumping), the diffusion length (typically on a micron scale), and the surface recombination velocity. The spatial distribution of minority carriers varies with the optical excitation energy leading to an excitation energy dependence of the luminescence spectra. Therefore, an unambiguous interpretation of these spectra requires an accurate consideration of the excitation conditions, the carrier kinetics and the escape mode of the luminescence radiation, providing a set of parameters for fitting the spectra. Usually, these parameters are not well known.

However, in crystals with high quantum efficiency of emission, the minority carrier distribution is strongly modified by the recycling effects (multiple emission-

reabsorption events)^{10–12}. When the losses of carriers (via non-radiative recombination) and photons (via residual free-carrier absorption) are low, the recycling leads to a dramatic increase of the minority-carrier spread in the sample⁹. This was found to be crucial for the correct interpretation of the difference between the observed spectra in the transmission and reflection geometries¹².

The giant spread of minority carriers (up to centimeter-scale distances at low T) makes it possible to study the luminescence spectra in a novel geometry, where the excitation is provided at an edge face of the sample and observation is carried out from the broadside^{13,14}. Thus observed spectra do not depend on the distance from the edge to the observation region in a wide range of distances, for differently doped samples, and at different temperatures, which implies a stable minority carrier distribution^{13,14}.

Here we present a study of the luminescence emission spectra for a moderately doped n -InP wafer, obtained with the edge-face excitation. Since the outgoing radiation is captured from the crystal region that is remote from the edge, the effective excitation in that region is predominantly by the radiation in the red wing of the emission spectrum, for which the wafer is mostly transparent. Therefore, the excitation spreads to a high extent homogeneously across the wafer. The main advantage of this geometry is a much simplified and more accurate account of the spectral filtering.

We report the temperature dependence of the spectra. At temperatures $T > 200$ K the spectra are close to those obtained with van Roosbroek-Shockley relation for the intrinsic emission spectrum. However for lower temperatures, the deviation is noticeable. We interpret this as due to non-equilibrium effects arising from the spatial fluctuations of the impurity potential.

EXPERIMENT

We studied moderately-doped n -InP wafers¹⁵ with the room-temperature Hall mobility of $3000 \text{ cm}^2/\text{Vs}$, comparable to mobilities previously reported for InP epitaxial films and crystals with similar doping concentrations⁶. The edge-excitation geometry illustrated in Fig. 1 al-

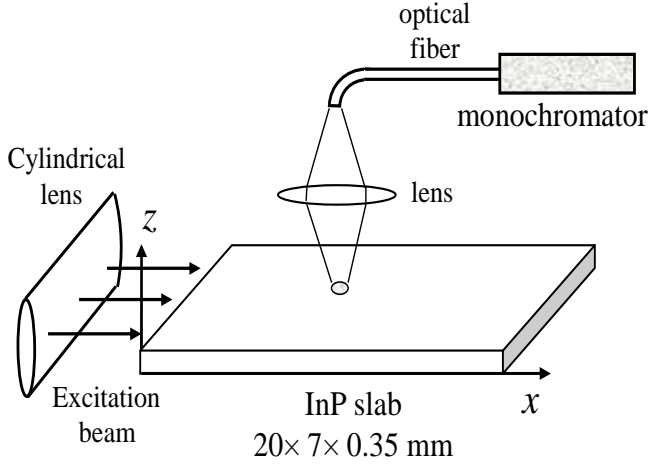


FIG. 1. (Color online) Schematics of the experimental geometry. An 808 nm excitation beam is focused on a $0.35 \times 7 \text{ mm}^2$ edge of the sample; the photoluminescence is registered from the broadside at varying x .

lowed us to study luminescence far away from the excitation region. The broadside luminescence was captured by a lens to image a small patch of the surface onto an optical fiber transmitting the light to the entrance slit of a monochromator. After passing through the output slit, the chopped and spectrally dispersed light beam illuminated a 1.1-cm Si-detector, connected to a lock-in amplifier. To account for the spectrally-dependent attenuation of light in the optical system as well for the spectral sensitivity of the detector, we scanned the spectrum of a halogen lamp, which is quite close to the black-body spectrum at $T = 2500 \text{ K}$ within the spectral range from 800 nm to 1100 nm. The obtained spectral response of the whole system with respect to the black-body radiation in this spectral range was used to correct the raw luminescence spectral scans and reconstruct the original luminescence spectra (Fig.2).

The absorption spectra and the luminescence spectra measured in a more traditional reflection geometry were also available for the same sample^{9,16,17}. We remark that the shapes of both absorption and luminescence spectra at room temperature had a negligible variation in the doping interval $n_d = 2 - 6 \times 10^{17} \text{ cm}^{-3}$, though the samples with $n = 3 \times 10^{17} \text{ cm}^{-3}$ had maximal brightness of emission and thus higher quantum efficiency¹⁸.

Luminescence spectra for $n = 3 \times 10^{17} \text{ cm}^{-3}$ sample at various temperatures measured at $x = 0.5 \text{ mm}$ are shown in Fig. 2. Also shown are the results of calculations discussed below. The spectra recorded at different distances x between the observation spot and the excitation edge in the range between $x = 0.2$ and 5 mm were all identical in shape. No variation with the excitation energy E_{ex} (for $E_{\text{ex}} > E_g$) was observed either.

The blue shift of the luminescence line clearly seen at lower temperatures is associated with the increasing band-gap. Also observed but less pronounced is some

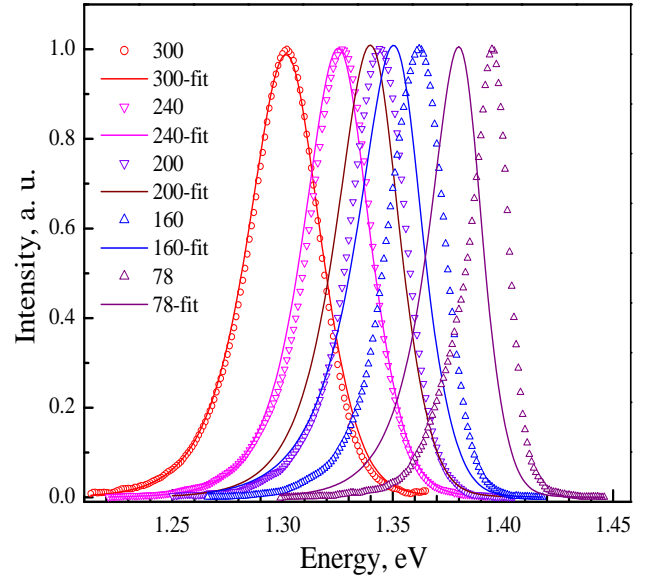


FIG. 2. (Color online) Edge excitation spectra at different temperatures (dots). Also shown (by solid lines) are results of calculations based on the intrinsic VRS spectrum (8).

narrowing of the line. The red wings of the lines at all temperatures closely follow an exponential decay law

$$I \propto \exp[(E - E_g)/\Delta'(T)] . \quad (1)$$

Similar exponential law with the same parameter $\Delta'(T)$ was observed in reflection-geometry experiments⁹.

DISCUSSION: EFFECTS OF SPECTRAL FILTERING

Because of the effects of self-absorption and multiple surface reflection, the luminescence spectra $I(E)$ observed from the broadside of a slab of finite thickness d are modified compared to the intrinsic emission spectra $S_i(E)$. The relation is of the form⁹:

$$I(E) = S_i(E)F(E) . \quad (2)$$

The function $F(E)$ describes the spectral filtering (reabsorption). It depends on the details of excitation and the observation geometry. Due to the high refractive index $n \approx 3.4$ of InP, the escape cone of luminescent radiation is narrow, and only radiation propagating perpendicular to the surface goes out. Therefore, the filtering function $F(E)$ can be expressed through a one-pass filtering function $F_1(E)$ for the light escaping to the sample surface,

$$F_1(E) = \int_0^d p(z) \exp[-\alpha(E)z] dz, \quad (3)$$

where $p(z)$ is the photo-generated hole concentration at a distance z from the surface (see Fig. 1). In our case, the distribution $p(z)$ is almost homogeneous along z and

symmetric relative to the mid-plane $z = d/2$. Taking into account multiple reflections of the luminescence radiation, we have⁹

$$F(E) = F_1 \frac{1 - R(E)}{1 - R(E) \exp(-\alpha d)}, \quad (4)$$

where $R(E)$ is the surface reflection coefficient (confidently assumed to be the same for both sample surfaces).

At large distances x from the excitation edge, the distribution $p(z)$ that appears in Eq. (3) is generated by weak reabsorption of red photons in the transparency region. Therefore it can deviate from a constant only in narrow depletion regions near surfaces, due to surface recombination,

$$p(z) = p_0[1 - c \exp(-z/l)], \quad (5)$$

where l is the width of the region with depleted minority carrier concentration. This width is analogous to the conventional diffusion length. If the surface recombination velocity s is fast, the constant c can be estimated as $c = sl/(sl + D) \leq 1$, where D is the diffusion coefficient of holes. Evidently, surface recombination effects will be noticeable in our geometry only in the spectral region where $\alpha(E)l \geq 1$ (i.e. in the far end of the blue wing of the observed line). In contrast, in the traditional reflection-geometry experiment this effect modifies the luminescence line along the whole blue wing starting from the line center. In the reflection geometry, the minority-carrier concentration rapidly decays away from the surface and the spectra are very sensitive to the shape of $p(z)$. That shape is defined by the kinetics of surface recombination and diffusion, as well as by specific conditions of the excitation. Both c and l are used in this work as (non-essential) fitting parameters.

Equation (2) suggests that the intrinsic emission spectrum can be recovered from the observed luminescence spectrum, so long as the filtering function is calculated with a sufficient accuracy. Let us now discuss the inherent limitations of this procedure.

The main limitation comes from an exponential growth of the absorption coefficient in the range of interest, leading to a steep variation of $F(E)$. The absorption spectra of direct bandgap semiconductors typically feature an Urbach-type energy dependence¹⁹ of the interband absorption extending at least from $\alpha = 1$ to 500 cm^{-1} . In our moderately doped InP samples this Urbach-tail region extends up to 5000 cm^{-1} for all T . One can evaluate the interband absorption coefficient deeper into the bandgap by subtracting the residual (free-carrier) absorption that is essentially constant in this energy region and grows linearly with the doping¹⁶. The interband absorption spectra for our sample are shown in Fig. 3 for $T=300 \text{ K}$ and $T = 78 \text{ K}$. For comparison and further discussion, we also show the absorption coefficient in the region of large absorption for a much lower-doped sample ($n = 5 \times 10^{15} \text{ cm}^{-3}$) from²⁰ exhibiting an excitonic feature near the absorption edge, as well as the relevant textbook data²¹ (where this feature is not resolved).

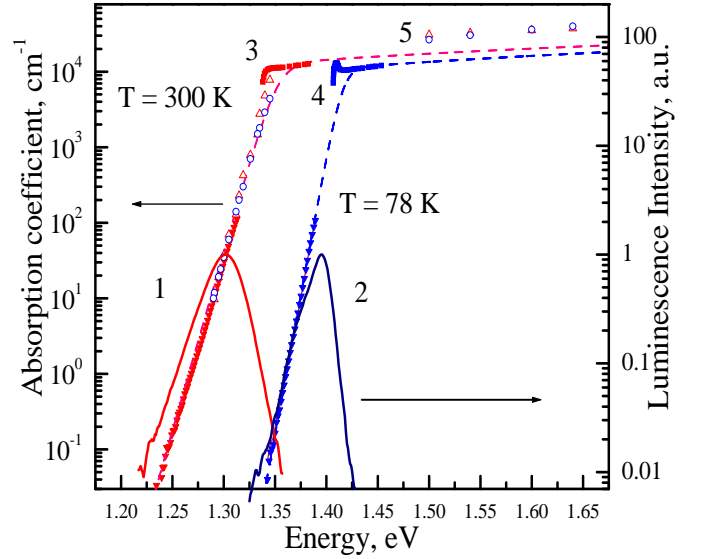


FIG. 3. (Color online) Luminescence spectra (log scale) observed at $T = 300 \text{ K}$ (1) and at $T = 78 \text{ K}$ (2) in the edge-excitation geometry; $n = 3 \times 10^{17} \text{ cm}^{-3}$. Also shown are the experimental absorption spectra from¹⁷, triangles, as well as the spectra for undoped InP (3) and (4) from²⁰, and (5) from²¹. Dashed lines show the interpolated absorption coefficient used in calculations of the luminescence spectra and the filtering functions.

Matching the experimental absorption spectra to the Urbach law,

$$\alpha = \alpha_0 \exp \left[\frac{E - E_g(n, T)}{\Delta(n, T)} \right], \quad (6)$$

[where $\Delta(n, T)$ is the Urbach tail parameter] with the well-known²² behavior of the bandgap energy $E_g(T)$ for undoped InP gives $\alpha_0 = 1.1 \times 10^4 \text{ cm}^{-1}$; this value provides a good fit in a wide temperature range $T = 0$ to 1000 K ²³. The physical interpretation of α_0 in Eq. (6) as the value of α at $E = E_g$ (i.e. above the steep slope region) suggests that α_0 should not vary with the concentration at a moderate doping level, $n \leq 10^{18} \text{ cm}^{-3}$, when the Fermi level is still below or near the conduction band edge. This allows us to further estimate both $E_g(n, T)$ and $\Delta(n, T)$ from the absorption spectra of our moderately n -doped sample. The results are shown in Fig. 4 together with the data obtained for semi-insulating InP²³. One can see that in the temperature interval $300 \geq T \geq 150 \text{ K}$ the values of $\Delta(n, T)$ are increased by $\approx 1.5 \text{ meV}$ as compared to the undoped sample, while the difference in $E_g(T, n)$ is minimal. Variations of both $E_g(n, T)$ and $\Delta(n, T)$ with the temperature and the doping can be described^{23,24} in the Einstein model for lattice vibrations,

$$\begin{aligned} E_g(n, T) &= E_{g,0} - \Delta E_g(n, T) - s_g k \theta [\coth(\theta/2T) - 1], \\ \Delta(n, T) &= s(n) + s_\Delta k \theta [\coth(\theta/2T) - 1], \end{aligned} \quad (7)$$

where θ is an effective Debye temperature, which for our

samples equals 270 K. This agrees with the values of θ for InP reported in the literature^{23,24} (they vary in the range $\theta = 240\text{--}310$ K, apparently depending on the crystal quality). The term $\Delta E_g(n, T)$ accounts for bandgap narrowing with the doping. Terms with s_g and s_Δ describe the effects of temperature and are proportional to the electron-phonon coupling constant. Term with $s(n)$ describes the effect of concentration on the Urbach tail parameter. Equations (7) imply that these two effects are statistically independent and can be included additively²⁵. The observed reduction of $s(n)$ at low temperatures is in line with reduction of the screening length of the random potential.

Based on the absorption spectrum, we note that for $E \geq E_g$ the region $z \geq 1/\alpha_0$ gives an exponentially small contribution to the integral in Eq. (3), while the experimentally known values of $\alpha(E)$ are not reliable. Therefore, in an attempt to recover the intrinsic spectrum from Eq. (2), the blue wing of the intrinsic emission spectrum cannot be accurately estimated. It is more consistent to perform a model calculation of the intrinsic spectrum and then compare with the experiment using Eq. (2). While this procedure is accurate, it gives no prejudice about the suppressed blue wing of the intrinsic spectrum.

DEVIATION FROM THERMAL EQUILIBRIUM

For a quasi-equilibrium carrier energy distribution (with different quasi-Fermi levels for electrons and holes) the intrinsic emission spectrum of semiconductor obeys the van Roosbroek-Shockley (VRS) relation²⁶,

$$S_i(E) = \alpha(E)E^3 \exp(-E/kT), \quad (8)$$

which allows one to calculate $S_i(E)$ using experimental data for the absorption spectrum. The calculated edge-excited luminescence spectra are presented in Fig. 2 by the solid lines. The calculation is based on the interpolated absorption coefficient⁹, shown in Fig. 3 for $T = 78$ K and 300 K. For not too low temperatures ($T \geq 200$ K), the spectra calculated from the intrinsic VRS spectra (8) provide an excellent fit to the shape of the observed line. The only fitting parameter is the surface depletion length l . Because of the recycling effects, one can anticipate somewhat enlarged values of l , compared to estimates based on typical surface recombination velocity and normal diffusion coefficient of holes, so that the fitting values in the range of 7 to 14 μm appear reasonable. We shall not be concerned with the more detailed interpretation of the parameter l because its influence is limited only to the far blue wing of the line and the experimental accuracy of the spectrum measurement (2) is insufficient in that region. The position of the line center can be calculated as in Ref.¹³. The line center energy is approximately described by $\alpha(E)d = 1$, which again shows that it is controlled by the filtering.

For $T \leq 200$ K the calculated lines no longer agree with the experiment. The experimental line maxima (Fig. 4)

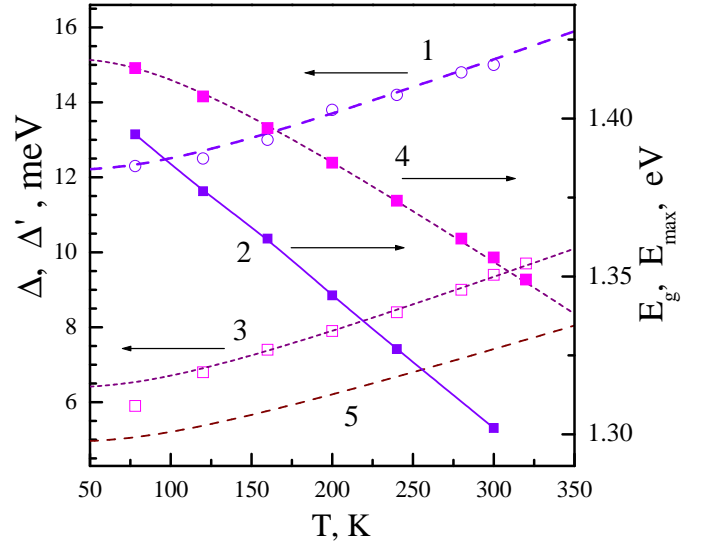


FIG. 4. (Color online) Temperature variation of the luminescence spectrum parameters for n -type InP sample, $n = 3 \times 10^{17} \text{ cm}^{-3}$. Curves (1) and (2) show, respectively, the red-wing exponential decay parameter Δ' and the position of the line maximum, E_{max} . Experimental data are indicated by the symbols while the dashed lines represent fit by Eqs. (7) with $\theta = 270$ K. Also shown are the Urbach tail parameter Δ (curve 3) and the bandgap E_g (curve 4) obtained from the absorption spectra. Curve 5 plots the Urbach tail parameter Δ for undoped InP, from Ref.²³.

are systematically at higher energies than those calculated from the VRS relation (8). At 78 K this discrepancy is about 13 meV.

Moreover, the relation between parameters Δ' and Δ expected¹⁷ from the VRS relation no longer holds at low temperatures. This relation is of the form

$$\frac{1}{\Delta'(n, T)} = \frac{1}{\Delta(n, T)} - \frac{1}{T}. \quad (9)$$

We find that for $T \leq 200$ K the values of $\Delta'(T)$ extracted from the spectra are smaller than those calculated from the red-wing slope of $\log \alpha$ with Eq. (9). This may suggest that holes have an effective temperature higher than the lattice temperature. At room temperature, the energy relaxation time τ_ϵ of holes is several orders of magnitude shorter than the radiative recombination time τ_{rad} . The ratio $\tau_{\text{rad}}/\tau_\epsilon$ is reduced at lower temperatures, since τ_{rad} gets shorter while the energy relaxation slows down. Still, the “hot hole” stationary state seems to be highly improbable. Nevertheless, the decreasing ratio $\tau_{\text{rad}}/\tau_\epsilon$ can have a profound effect in reducing the spectral filtering. Such a reduction was experimentally observed²⁷ in the standard reflection geometry for low-temperature (78 K and below) emission from InSb. Quantitative account of this effect requires a separate study, but qualitatively it would explain the blue shift of the experimental line maxima at low temperatures compared to their position calculated using Eq. (3).

Accounting for a discrepancy with the VRS relation requires understanding of how non-equilibrium enters the picture. As already mentioned, we consider unlikely a homogeneous ensemble of holes characterized by an elevated effective temperature, because that would require a physically unrealistic small ratio $\tau_{\text{rad}}/\tau_e \approx 1$.

A more likely candidate for a non-equilibrium stationary state of holes at low temperatures is associated with the spatial fluctuations^{28–30} in doping concentration and the resultant local potential fluctuations. The ionized donors repel the holes thus increasing their potential energy. A local depletion of the donor concentration provides a potential well from which holes recombine. The recombination process is faster than that of spatial exchange of holes between different wells and therefore does not have to obey the VRS relation.

Moreover, since the lower doping results in lower values of the Urbach parameter $\Delta(n, T)$ in absorption spectra, the local decrease of doping should lead to smaller values of $\Delta'(T)$. One can use this observation to check whether a local decrease of concentration of ionized donors is sufficient to interpret the observed variation of $\Delta'(n, T)$. The required fluctuations of n can be estimated from Eqs. (9) and (7), which incorporate the experimental values of $\Delta'(n, T)$ and $\Delta(n, T)$. For $T=78$ K we find that the local concentration drop by an order of magnitude is sufficient to explain the observed value of $\Delta'(n, T)$ — without assuming an elevated effective hole temperature.

The local concentration drop can also explain the low-temperature blue shift of the luminescence maxima. The locally low-doped areas of the sample do not experience the bandgap narrowing effect that could be estimated for homogeneous doping^{6,31}. Precise values of the narrowing are still a matter of discussion and apparently depend on

the experimental conditions for observation. According to optical experiments of Ref.^{6,24}, the bandgap narrowing in n -InP is well approximated by $\Delta E_g(n) = -c (n \times 10^{-18})^{1/3}$ meV. For $T = 78$ K the constant $c = 71.4^6$, giving an estimate of $\Delta E_g \approx 20$ meV for the depleted fluctuation region. We see that the effect is even larger than that needed to account for the blue shift of the luminescence lines at $T = 78$. For $T = 300$ K one has $c = 22.5$ and the narrowing effect is reduced²⁴. Besides, the system at $T = 300$ is much closer to equilibrium.

CONCLUSIONS

In summary, we have presented a novel photoluminescence geometry, with edge excitation and broad-side observation. We show that this geometry has no sensitivity to the excitation energy and little sensitivity to the surface conditions. It is therefore well suited for the characterization of intrinsic emission spectra. For not too low temperatures, $T \geq 200$ K the measured spectra agree with those calculated on the basis of the van Roosbroek-Shockley relation. For $T \leq 200$ K, the observed spectra deviate from VRS. This deviation is attributed to spatial fluctuations in the doping concentration in our moderately doped InP samples, giving rise to a non-equilibrium distribution of minority carriers.

This work was supported by the Defense Threat Reduction Agency through its basic research program and by the New York State Office of Science, Technology and Academic Research through the Center for Advanced Sensor Technology at Stony Brook.

* Corresponding author, arsen.subashiev@stonybrook.edu

¹ L. Pavesi and M. Guzzi, “Photoluminescence of $\text{Al}_x\text{Ga}_{1-x}\text{As}$ alloy,” J. Appl. Phys. 75 (1994) 4779.

² Y. Zhang, A. Mascarenhas, J. F. Geisz, H. P. Xin, and C. W. Tu, “Discrete and continuous spectrum of nitrogen-induced bound states,” Phys. Rev. B 63 (2001) 085205.

³ A. Haufe, R. Schvabe, H. Fieseler, and M. Ilegems, “The luminescence lineshape of highly doped direct-gap III-V compounds,” J. Phys. C: Sol. St. Phys. 21 (1988) 2951.

⁴ C. J. Hwang, “Optical Properties of n-Type GaAs. I. Determination of Hole Diffusion Length from Optical Absorption and Photoluminescence Measurements,” J. Appl. Phys. 40 (1969) 3731.

⁵ D. Gershoni, H. Temkin, G. J. Dolan, J. Dunsmuir, S. N. G. Chu, and M. B. Panish, “Effects of two-dimensional confinement on the optical properties of InGaAs/InP quantum wire structures,” Appl. Phys. Lett. 53 (1988) 995.

⁶ R. M. Sieg and S. A. Ringel, “Reabsorption, band-gap narrowing and the reconciliation of photoluminescence spectra with electrical measurements for epitaxial InP,” J. Appl. Phys. 80 (1996) 448.

⁷ H. Barry Bebb and E. W. Williams, “Photoluminescence

1: theory”, in: R. K. Willardson and A. C. Beer (Eds.), Semiconductors and Semimetals, vol. 8, Academic, New York, 1972, p. 182.

⁸ O. von Roos, “Influence of radiative recombination on the minority carrier transport in direct band-gap semiconductors,” J Appl. Phys. 54 (1983) 1390.

⁹ O. Semyonov, A. Subashiev, Z. Chen, and S. Luryi, “Photon assisted Lévy flights of minority carriers in n-InP,” J. Luminesc. 132 (2012) 1935.

¹⁰ P. Asbeck, “Self-absorption effects on the radiative lifetime in GaAs - GaAlAs double heterostructures,” J. Appl. Phys. 48 (1977) 820.

¹¹ V.V. Rossin and V.G. Sidorov, “Reabsorption of Recombination Radiation in Semiconductors with High Internal Quantum Efficiency,” Phys. Stat. Solidi (a) 95 (1986) 15.

¹² S. Luryi and A. V. Subashiev, “Lévy Flight of Holes in InP Semiconductor Scintillator,” Int. J. High Speed Electron. Syst. 21 (2012) 1250001; online at <http://arXiv.org/pdf/1202.5576>.

¹³ S. Luryi, O. Semyonov, A. V. Subashiev, Z. Chen, “Direct observation of Lévy flights of holes in bulk n -doped InP,” Phys. Rev. B 86 (2012) 201201(R) .

- ¹⁴ A. Subashiev, O. Semyonov, Z. Chen, and S. Luryi, "Temperature controlled Lévy flights of minority carriers in photoexcited bulk n -InP," in press (2013); online at <http://arXiv.org/pdf/1302.4399>.
- ¹⁵ Sulfur-doped ACROTEC InP wafers from NIKKO Metals (Japan).
- ¹⁶ O. Semyonov, A. Subashiev, Z. Chen, and S. Luryi, "Radiation efficiency of heavily doped bulk n -InP semiconductor," J. Appl. Phys. 108 (2010) 013101.
- ¹⁷ A. Subashiev, O. Semyonov, Z. Chen, and S. Luryi, "Urbach tail studies by luminescence filtering in moderately doped bulk InP," Appl. Phys. Lett. 97 (2010) 181914.
- ¹⁸ Heavier doping results in two additional effects that lie outside our present scope. The emission spectra are modified by the conduction-band filling and smearing of the interband absorption edge. The absorption spectra are masked in the tailing region by the residual free-carrier absorption.
- ¹⁹ F. Urbach, "The Long-Wavelength Edge of Photographic Sensitivity and of the Electronic Absorption of Solids," Phys. Rev. 92 (1953) 1324.
- ²⁰ W. J. Turner, W. E. Reese, and R. S. Petit, "Exciton absorption and emission in InP," Phys. Rev. A 136 (1964) 1467.
- ²¹ Handbook of Optical Constants of Solids, ed. E. Palik (Academic Press, New York, 1985); also S. Adachi, Optical Constants of Crystalline and Amorphous Semiconductors (Kluwer Academic, Boston, 1999).
- ²² I. Vurgaftman, J. R. Meyer, and L. R. Ram-Mohan, "Band parameters for III-V compound semiconductors and their alloys," J. Appl. Phys. 89 (2001) 5815.
- ²³ M. Beaudoin, A. J. G. DeVies, S.R. Johnson, H. Laman, and T. Tiedje, "Optical absorption edge of semi-insulating GaAs and InP at high temperatures," Appl. Phys. Lett. 70 (1997) 30.
- ²⁴ S. Y. Chung, D. Y. Lin, Y. S. Huang, K. K. Tiong, "Piezoreflectance study of InP near the absorption edge," Semicond. Sci. Technol. 11 (1996) 1850.
- ²⁵ S. John, C. Soukoulis, M. H. Cohen, and E. N. Economou, "Theory of electron band tails and the Urbach Optical Absorption Edge," Phys. Rev. Lett. 57 (1986) 1777.
- ²⁶ W. van Roosbroek and W. Shockley, Phys. Rev. 94 (1954) 1558; the relation is sometimes referred to as the Kubo-Martin-Schwinger theorem, cf. R. Kubo, J. Phys. Soc. Jpn. 12 (1957) 570; P. C. Martin and J. Schwinger, Phys. Rev. 115 (1959) 1342.
- ²⁷ A. Mooradian and H. Y. Fan, "Recombination emission in InSb," Phys. Rev. 148 (1966) 873.
- ²⁸ Spatial fluctuations of the band edges in homogeneously-doped semiconductors have been proposed to explain deviations of low-temperature photoluminescence spectra from the VRS shape both in bulk crystals (with assumed Gaussian absorption tails)²⁹ and quantum wells³⁰.
- ²⁹ P.G. Eliseev, "Anti-Stokes luminescence in heavily doped semiconductors as a mechanism of laser cooling," Opto-Electron. Rev. 16 (2008) 199; also P.G. Eliseev, "The red σ^2/kT spectral shift in partially disordered semiconductors," J. Appl. Phys. 93 (2003) 5404.
- ³⁰ S. Chatterjee, C. Ell, S. Mosor, G. Khitrova, H. M. Gibbs, W. Hoyer, *et al.*, "Excitonic Photoluminescence in Semiconductor Quantum Wells: Plasma versus Excitons," Phys. Rev. Lett. 92 (2004) 067402.
- ³¹ G. Borghs, K. Bhattacharyya, K. Deneffe, P. VanMieghem, and R. Mertens, "Band-gap narrowing in highly doped n - and p -GaAs studied by photoluminescence spectroscopy," J. Appl. Phys. 66 (1989) 4381.